Environmental Science & Technology

Article

pubs.acs.org/est

Contribution of Brown Carbon to Direct Radiative Forcing over the Indo-Gangetic Plain

P. M. Shamjad,[†] S. N. Tripathi,*[,†] Ravi Pathak,[‡] M. Hallquist,[‡] Antti Arola,[§] and M. H. Bergin[∥]

[†]Department of Civil Engineering, and Centre for Environmental Science and Engineering, Indian Institute of Technology Kanpur, Kanpur, India

[‡]Atmospheric Science, Department of Chemistry and Molecular Biology, University of Gothenburg, SE-41296 Gothenburg, Sweden

[§]Finnish Meteorological Institute, P.O. Box 1627, 70211 Kuopio, Finland

[∥]School of Earth and Atmospheric Sciences, Georgia Institute of Technology, Atlanta, Georgia, United States

Supporting Information

ABSTRACT: The Indo-Gangetic Plain is a region of known high aerosol loading with substantial amounts of carbonaceous aerosols from a variety of sources, often dominated by biomass burning. Although black carbon has been shown to play an important role in the absorption of solar energy and hence direct radiative forcing (DRF), little is known regarding the influence of light absorbing brown carbon (BrC) on the radiative balance in the region. With this in mind, a study was conducted for a one month period during the winter−spring season of 2013 in Kanpur, India that measured aerosol chemical and physical properties that were used to estimate the sources of carbonaceous aerosols, as well as parameters necessary to estimate direct forcing by aerosols and the contribution of BrC absorption to the atmospheric energy balance. Positive matrix factorization analyses, based on aerosol mass spectrometer measurements, resolved organic carbon into four factors including low-volatile oxygenated organic aerosols, semivolatile oxygenated organic aerosols, biomass burning, and hydrocarbon like organic aerosols. Three-wavelength absorption and scattering coefficient measurements from a Photo Acoustic Soot Spectrometer were used to estimate aerosol optical properties and estimate the relative contribution of BrC to atmospheric absorption. Mean ± standard deviation values of short-wave cloud free clear sky DRF exerted by total aerosols at the top of atmosphere, surface and within the atmospheric column are −6.1 ± 3.2, −31.6 ± 11, and 25.5 ± 10.2 W/m^2, respectively. During days dominated by biomass burning the absorption of solar energy by aerosols within the atmosphere increased by ∼35%, accompanied by a 25% increase in negative surface DRF. DRF at the top of atmosphere during biomass burning days decreased in negative magnitude by several W/m^2 due to enhanced atmospheric absorption by biomass aerosols, including BrC. The contribution of BrC to atmospheric absorption is estimated to range from on average 2.6 W/m^2 for typical ambient conditions to 3.6 W/m^2 during biomass burning days. This suggests that BrC accounts for 10−15% of the total aerosol absorption in the atmosphere, indicating that BrC likely plays an important role in surface and boundary temperature as well as climate.

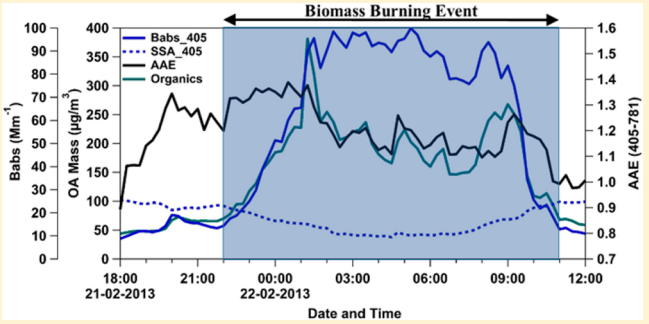

INTRODUCTION

Aerosols in the atmosphere affect the Earth's radiative budget both directly by scattering and absorbing solar radiation and indirectly by influencing cloud albedo and lifetime.[1] The impact of black carbon (BC) on the Earth's radiative budget has been extensively studied due to its light absorbing properties. BC is known to absorb light throughout the light spectrum and thereby heat the atmosphere.[2] In addition to BC, the atmosphere also contains light absorbing organic aerosols (OA) known as brown carbon (BrC).[3] Several studies reported BrC aerosols with optical absorbing capacity varying from 15 to 50% of total aerosols.[4−6] Dust is another aerosol component present in the atmosphere capable of absorbing light.[4]

The sampling location for this study is Kanpur India, a representative site located within the Indo-Gangetic Plain (IGP). The IGP is designated as one of the most polluted regions in the world with very high aerosol loadings. Kanpur has a population of over 4.5 million with a density of 1452 people/km^2.[7] Major sources of aerosols in the IGP consist of domestic, industrial, and vehicular emissions. Kanpur also receives aerosols through long-range transport from the northwestern part of India. During the winter−spring months (December to March) IGP has large scale biomass burning coupled with high relative humidity (RH) conditions, resulting in heavy fog and haze.[8] These fog events last from several hours

Received: February 24, 2015
Accepted: August 3, 2015
Published: August 3, 2015

DOI: 10.1021/acs.est.5b03368
Environ. Sci. Technol. 2015, 49, 10474−10481

to a few days disrupting traffic and causing heath issues to humans.

Anthropogenic activities such as burning of fossil fuels and biomass emit large amounts of BC and OA along with other species into the atmosphere. Open biomass burning, such as crop residue burning, is considered to be a large source for BC and BrC.[3] Although BrC is coemitted with BC during biomass burning, there are other pathways, such as photochemical reactions, which can also lead to increased BrC in the atmosphere.[9] There is large spatial and temporal variation in sources and chemical properties of BrC as well as chemical, optical, and microphysical properties of BrC that have yet to be fully characterized. Also, the hygroscopic nature of BrC changes its optical properties with RH. All of these factors make estimating the radiative forcing involving BrC aerosols very difficult.

Detailed knowledge of aerosols' physical and chemical characteristics, along with their inter-relationship is required to calculate the net radiative budget of Earth due to aerosols. Bond et al.[4] report a global Direct Radiative Forcing (DRF) value of 1.1 ± 0.9 W/m^2 (mean ± standard deviation) for BC, which is the second largest climate forcer after CO_2. Very few studies are reported on the forcing due to BrC alone. One such study[5] reports a positive total forcing (3 to 4 W/m^2) at TOA for regions dominated by large scale indoor and outdoor biomass burning, like that in China, Africa, and IGP. Another study,[10] conducted at a local scale with measured optical properties, reports a 20% increase in forcing at the TOA when BrC is included in the forcing calculation.

The overall goal of this study is to estimate the relative contribution of BrC to direct radiative forcing over the IGP as well as to estimate the sources of light absorbing BrC. We discuss the optical properties of aerosols during late winter−spring season (February−March). Frequent biomass burning was observed during this study, which in turn produced large amounts of BC and primary/secondary OA. Since absorbing BrC is a subset of OA, it is expected that resolving OA into different factors can provide insight into chemical nature of BrC.

EXPERIMENTAL SECTION

Sampling Details. This study reports aerosol optical, chemical, and microphysical properties measured during 12 February to 20 March, 2013. Experiments were carried out in the Indian Institute of Technology-Kanpur (IIT-K) campus. Kanpur is located in the IGP, with a large urban population and poor air quality. Pollution sources in Kanpur are of mixed origin including vehicular, indoor and outdoor biomass burning, and industrial.[8] The period of study (February−March) is the late winter−spring season, which is associated with high RH (up to 85%) and low temperature (~10 °C).

Instrumentation. Instruments were operated continuously during the campaign. BC mass concentrations were measured using an Aethalometer (AE 42, Magee Scientific) operating at 2 L min^{-1} flow rate. Aa aethalometer measures light attenuation at seven wavelengths (370, 470, 520, 590, 660, 880, and 950 nm) with 5 min frequency which were then converted to BC mass concentration using a wavelength dependent specific attenuation factor. The mass concentration estimated at 880 nm is taken as the BC mass in this study. The BC mass concentration from the Aethalometer was corrected for filter loading and multiple scattering effects, as described elsewhere.[11,12] Absorption and scattering coefficients (B_{abs} and B_{scat}) of atmospheric aerosols were measured using Droplet Measurement Technology (DMT) three-wavelength Photo Acoustic Soot Spectrometer (PASS-3).[13,14] B_{abs} and B_{scat} were measured with a frequency of 0.5 Hz at three wavelengths,405, 532, and 781 nm, using a flow rate of 1 L min^{-1}. The PASS-3 was calibrated before and midway between the sampling study. An Aerodyne HR-ToF-AMS was used to determine the mass concentrations of organic and inorganic species in atmospheric aerosols.[15] HR-ToF-AMS can determine the mass concentrations of total organic carbon and nonrefractory species like ammonium, sulfate, nitrate, and chloride. It employs thermal heating (~600 °C) followed by electron ionization technique (70 eV) for the measurements of above species. The mass distribution of the above species with respect to their size was also measured by HR-ToF-AMS. HR-ToF-AMS measured mass spectra every second and produced an average spectrum every 2 min. Ionization efficiency calibrations were performed on HR-ToF-AMS before and after the campaign. The photoacoustic technique used in PASS 3 is known to have error in B_{abs} and B_{scat} at high RH conditions.[16] Also, the collection efficiency (CE) for HR-ToF-AMS may change according to the water content in the aerosol stream.[17] To minimize such errors, aerosols were dried (RH < 10%) before entering the PASS 3 and HR-ToF AMS using a silica gel dryer. Other than the above-mentioned instruments, this study also makes use of Level 2.0 aerosol optical depth (AOD_{Total}), single scattering albedo (SSA_{Total}), and asymmetry parameter (g_{Total}) from the Aerosol Robotic Network (AERONET) station located inside the IIT-K campus.[18] Daily 500 m resolution gridded seven wavelength surface albedo data from Moderate Resolution Imaging Spectro-radiometer (MODIS) was also used. Level 3 AOD from MODIS was used whenever AERONET data were not available. Each instrument's data were averaged to 15 min for analysis. Values from AERONET and MODIS were taken as daily average. Optical properties such as Absorption Angstrom Exponent (AAE) and Single Scattering Albedo (SSA) were calculated from PASS 3 measured spectral absorption. Overall, AAE is calculated from campaign average B_{abs} and B_{scat} and SSA from daily average B_{abs} and B_{scat}.

METHODS

Data Analysis. Unit mass resolution (UMR) data from HR-ToF-AMS was analyzed using the Squirrel (Version 1.54) software package and high resolution (HR) data were analyzed using PIKA (Version 1.13) assuming a collection efficiency of 0.5 for all species.[19] Flow correction and air beam corrections were performed on the data. Masses of organic carbon and other inorganic species were derived after fitting V mode mass to charge ratios (m/z) up to 150 in PIKA. Positive matrix factorization (PMF) was carried out on HR data using PMF evaluation tool (PET, Version 2.06) as explained elsewhere.[20] Percentage of the biomass burning indicator (f_{60}), defined as the ratio of m/z 60 to total organic mass, is used to identify biomass burning episodes. Days with f_{60} values higher than one standard deviation from the campaign average are considered as biomass burning days.

Modeling Framework. DRF was calculated using the Santa Barbara Discrete Ordinate Radiative Transfer (SBDART) model.[21] SBDART assumes plane-parallel radiative transfer based on the discrete ordinate approach. Radiative fluxes are integrated with Discrete Ordinate Radiative Transfer (DISORT) module.[22] Aerosol radiative forcing (ΔF) was calculated

DOI: 10.1021/acs.est.5b03368
Environ. Sci. Technol. 2015, 49, 10474−10481

from the difference in fluxes for an aerosol free atmosphere to aerosol laden atmosphere. ΔF were obtained at the top of atmosphere (ΔF_{TOA}), surface (ΔF_S), and atmosphere (ΔF_A) assuming clear sky conditions for the shortwave (0.25 to 4 μm) range. Clear sky conditions assume a cloud-free sky with all radiatively active molecular species in the Earth's atmosphere for both biomass burning and normal days. ΔF_A was the difference between ΔF_{TOA} and ΔF_S.

Inputs into SBDART to calculate total aerosol DRF are AOD_{Total}, SSA_{Total}, and g_{Total} along with spectral surface albedo. Out of 34 days of measurement, only 13 days of spectral SSA from AERONET were available. So we used SSA derived from daily average absorption and scattering measured by PASS 3 ($SSA_{\lambda\_PASS\ 3}$) throughout. ΔF_{TOA} and ΔF_S were calculated for solar zenith angles (SZA) from 0° to 90° with 5° increment and diurnally averaged forcing was given as follows:

$$\Delta F_{TOA/S} = \frac{1}{2}\int_0^1 \Delta F(\mu_0)\mathrm{d}\mu_0 \quad (1)$$

where μ_0 is the cosine of SZA.

An important aspect of this study is to calculate the specific influence of BrC on DRF. Optical properties of BrC aerosols were derived from measured parameters. AOD due to BrC was calculated as per the procedure given in Chung et al.[5] Previous studies[23] show very little presence of dust during the winter season in the IGP. So we assume the contribution of dust to be negligible. This study uses a modified form of eq 2 from Chung et al.[5] for deriving AOD for BrC as given below:

$$\mathrm{AAOD}_{\lambda o\_Total} \times \left(\frac{\lambda}{\lambda o}\right)^{-\mathrm{AAE}_{Total}} = \mathrm{AAOD}_{\lambda o\_BC} \times \left(\frac{\lambda}{\lambda o}\right)^{-\mathrm{AAE}_{BC}} + \mathrm{AAOD}_{\lambda o\_BrC} \times \left(\frac{\lambda}{\lambda o}\right)^{-\mathrm{AAE}_{BrC}} \quad (2)$$

where $\mathrm{AAOD}_{\lambda o\_Total}$, $\mathrm{AAOD}_{\lambda o\_BC}$ and $\mathrm{AAOD}_{\lambda o\_BrC}$ are the absorption AOD of total aerosols, BC and BrC, respectively, at a reference wavelength λ_0 of 532 nm. $\mathrm{AAOD}_{\lambda o\_Total}$ is calculated from AOD_{Total} using following equation:

$$\mathrm{AAOD}_{\lambda o\_Total} = AOD_{\lambda o\_Total} \times (1 - \mathrm{SSA}_{\lambda o}) \quad (3)$$

where AAE_{Total}, AAE_{BC}, and AAE_{BrC} are the Absorption Angstrom Exponent for total aerosols, BC and BrC, respectively. AAE_{BC} = 1 is assumed as reported in several studies.[6,24] AAE_{Total} and AAE_{BrC} were calculated using equation no. 4.

$$\mathrm{AAE} = \frac{-\ln\left(\frac{B_{abs\_\lambda 1}}{B_{abs\_\lambda 2}}\right)}{\ln\left(\frac{\lambda 1}{\lambda 2}\right)} \quad (4)$$

where $B_{abs\_\lambda 1}$ and $B_{abs\_\lambda 2}$ are absorption coefficients measured at $\lambda 1$ and $\lambda 2$ (405 and 781 nm in this study). The AAE_{Total} derived from spectral absorbance measured by PASS 3 has an average of 1.2 ± 0.2. AAE_{BrC} was calculated from spectral absorption coefficients derived by Mie code[25] developed by Bond et al.[26,27] For AAE_{BrC}, mass size distribution from HR-ToF-AMS was converted to number size distribution by assuming a density of 1.2 g cm^{-3}.[6] This size distribution along with RI for organic aerosols from Kirchstetter et al.[6] was used as input to Mie code to calculate spectral absorption of BrC. Average values for AAE_{BrC} was found to be 6.6 ± 0.3. Another recent study[28] reports an average AAE_{BrC} values of 9 ± 3 when measured using filter extracts. SSA for BrC was also calculated using Mie code. AAE_{BC} and AAE_{BrC} were used as input to eq 2 which was solved at 532 and 781 nm for $\mathrm{AAOD}_{\lambda o\_BC}$ and $\mathrm{AAOD}_{\lambda o\_BrC}$. AAOD for BC and BrC at 405 and 781 were then calculated using eq 5:

$$\mathrm{AAOD}_{\lambda\_BC/BrC} = \mathrm{AAOD}_{\lambda o\_BC/BrC} \times \left(\frac{\lambda}{\lambda o}\right)^{-\mathrm{AAE}_{BC/BrC}} \quad (5)$$

As SBDART requires AOD instead of AAOD, AOD for BrC is calculated using eq 3 with SSA for BC and BrC. Table 1 shows the average model input values used to calculate DRF for total aerosol and BrC at 532 nm.

Table 1. Average Values of Aerosol Optical Properties Used As Model Inputs at 532 nm

parameter	total aerosol DRF	BrC DRF
AOD	0.42 ± 0.17	0.02 ± 0.01
SSA	0.87 ± 0.03	0.83 ± 0.004
g	0.64 ± 0.04	0.67 ± 0.01
AAE_{Total}	1.2 ± 0.2	
AAE_{BrC}	6.6 ± 0.3	

RESULTS AND DISCUSSION

Diurnal Trend in Aerosol Properties. A strong diurnal variation in aerosol properties was observed throughout the sampling period. Figure 1 shows the diurnal variation of aerosol spectral absorption coefficients, BC and OA mass concentrations. Absorption at 405 nm was highest followed by 532 and 781 nm being the lowest throughout. AAE_{Total} value of 1.2 ± 0.2 suggests internally mixed BC and/or presence of BrC.[6,29,30] A sudden decline was observed in absorption coefficients and mass concentrations in the early morning around 5:30 am and a peak around 8:00 am, which can be attributed to the dilution effect due to the expansion of the atmospheric boundary layer and the increased emissions due to morning traffic and cooking.

PMF Factors. In order to infer sources of light absorbing carbon, PMF analysis of OA measured by HR-ToF-AMS was resolved into 4 distinct factors. We have followed Jimenez et al.[31] in identifying the less and more oxygenated factors of OA. The factors are identified as Low-Volatile Oxygenated Organic Aerosols (LV-OOA), Semi-Volatile Oxygenated Organic Aerosols (SV-OOA), Biomass Burning Organic Aerosols (BBOA), and Hydrocarbon like Organic Aerosols (HOA). (For more details on the PMF factor determinations see Supporting Information). Figure 2 shows the diurnal variation of PMF factors and Babs at 405 nm. All PMF factors, except SV-OOA, show a distinct diurnal trend. The diurnal change in SV-OOA mass is much smaller than other factors. LV-OOA was highest throughout the day followed by BBOA. Burning of wood, garbage, and dead leaves in the winter−spring season at sampling site produces large amounts of primary OA and secondary organic aerosols (SOA), similar to SV-OOA, which likely transforms to LV-OOA with photochemical aging.[31] An insignificant change in SV-OOA mass indicates its steady production throughout the sampling period. Sharp increases in BBOA and HOA during morning and evening hours can be attributed to cooking and vehicular traffic. LV-OOA attains a maximum roughly an hour later than that of BBOA and HOA suggesting the role of photochemistry in LV-OOA formation.

DOI: 10.1021/acs.est.5b03368
Environ. Sci. Technol. 2015, 49, 10474−10481

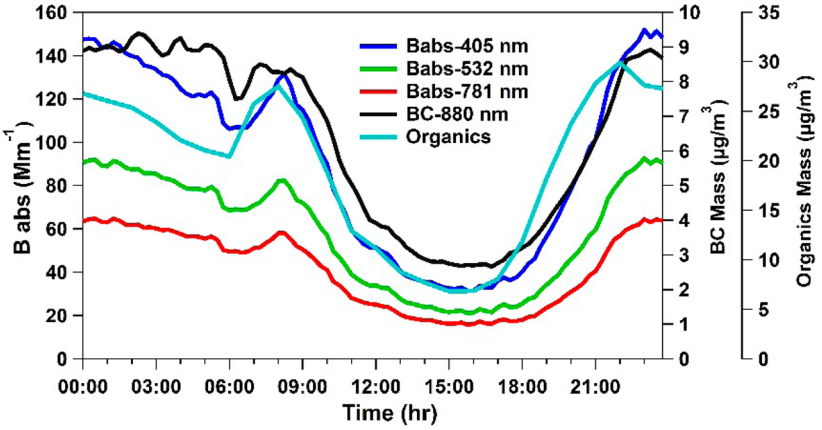

Figure 1. Diurnal variation of aerosol spectral absorption coefficients, BC and OA mass concentrations.

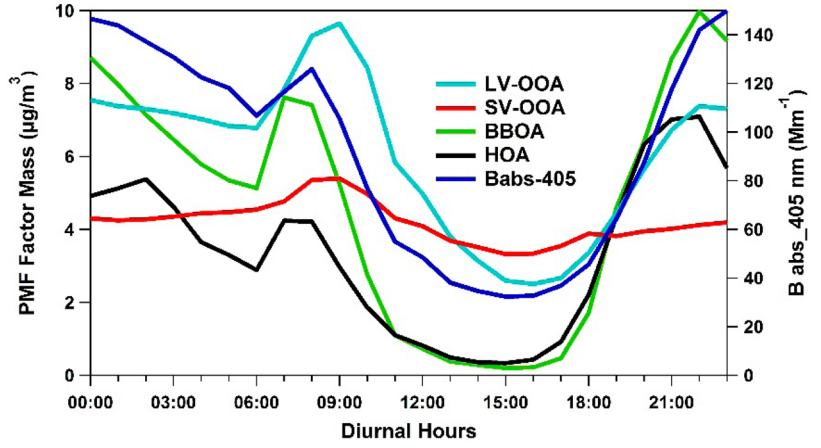

Figure 2. Diurnal variation of each PMF factor and Babs at 405 nm.

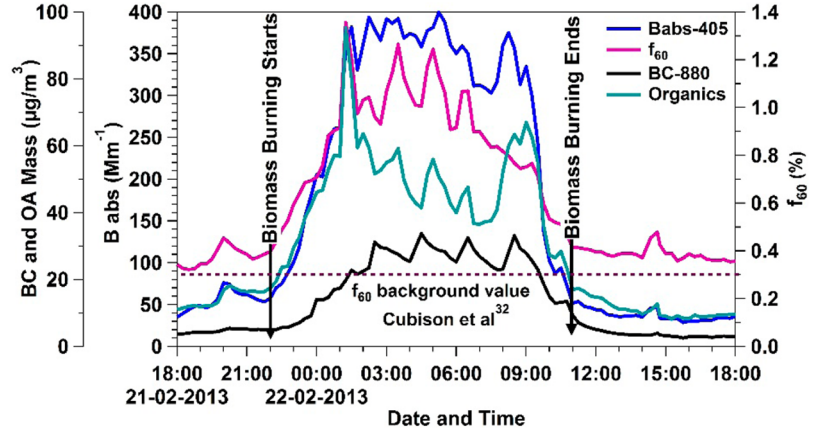

Figure 3. Spectral absorption, total organic mass, BC mass, and f_{60} for a typical biomass burning event on February 21st.

Changes in Aerosol Optical Properties during Biomass Burning Events. During the campaign, 7 biomass burning episodes were identified. Each biomass burning period was characterized by a sharp increase in BC and OA concentrations and increases in spectral absorption coefficients. Figure 3 shows a time series of spectral absorption coefficients, total organic mass, BC mass, and f_{60} for a typical 12 h biomass burning event started on February 21st. The background value of f_{60} was slightly higher (0.4%) than what was reported in earlier studies (0.3%).[32] During biomass burning events f_{60} value was as high as 1.3%.

BC, OA mass concentrations, and B_{abs} values measured during biomass burning events in this study are similar in trend but higher in magnitude when compared to previous studies.[33,34] Figure 4 shows the AAE and SSA values for the same biomass burning period as in Figure 3. Considerable differences were observed in SSA and AAE trends and values when compared to Lack et al.[33] AAE values of 2.3 were reported by Lack et al. but this study shows AAE of 1.2 ± 0.2.

DOI: 10.1021/acs.est.5b03368
Environ. Sci. Technol. 2015, 49, 10474−10481

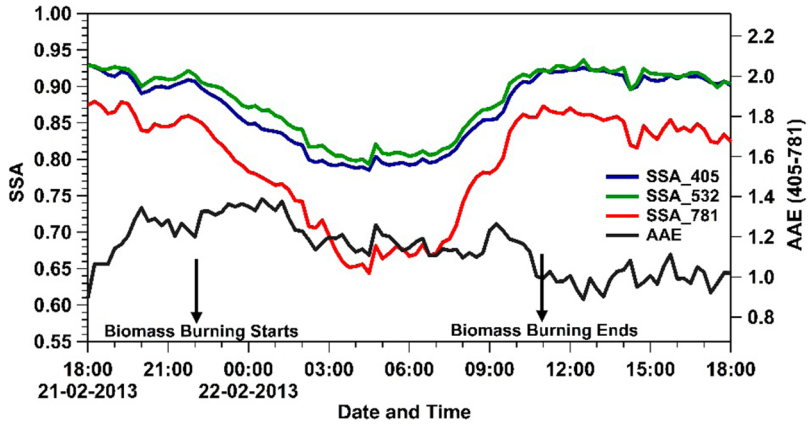

Figure 4. Spectral SSA and AAE for February 21st biomass burning event.

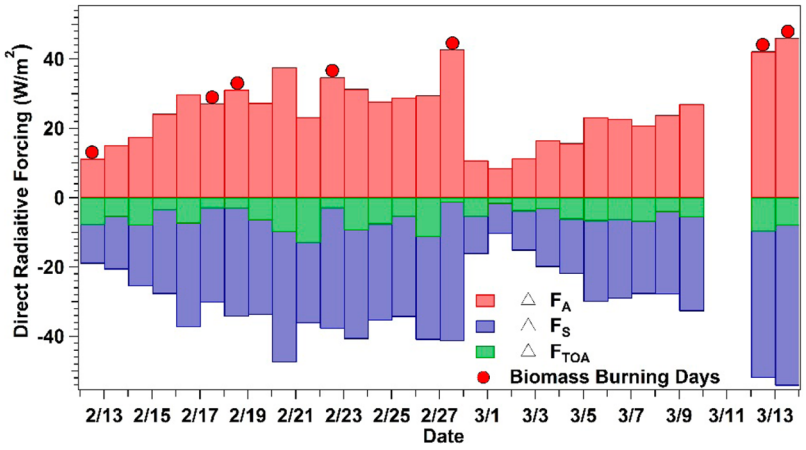

Figure 5. Total short wave clear sky aerosol direct radiative forcing for TOA (ΔF_{TOA}), surface (ΔF_S), and atmosphere (ΔF_A).

Table 2. Summary of DRF Values (W/m^2)

	total aerosol DRF		BrC DRF	
location	normal	biomass burning	normal	biomass burning
TOA	−6.6 ± 2.6	−4.5 ± 4	−1.1 ± 0.4	−1.0 ± 0.7
surface	−29.5 ± 9	−38.9 ± 11	−3.6 ± 1.4	−4.6 ± 1.9
atmosphere	22.1 ± 7	34.5 ± 12	2.6 ± 1.0	3.6 ± 1.5

Also SSA values in Lack et al. show increases during biomass burning, but this study shows decreases. These changes could indicate the presence of large quantities of BC and/or highly absorbing BrC coupled with mixing in the biomass burning plume sampled in this study. Lack et al.[33] reported a biomass burning event that happened due to wildfire on pine forest in Colorado, U.S.A. As the winter−spring time biomass burning in the IGP consists of materials with mixed origins such as garbage, wood, and vegetation, the resultant plume may not exhibit unique characteristics as that of wildfires. Low AAE values might be due to the large scale aging process during the transport of the plume to the sampling location. Another factor affecting the optical properties of biomass burning aerosols are the temperatures of burning. Since most of the biomass burning in the IGP are open burning, once the flames go out, the remaining fuel smolders for a long time, producing continuous smoke. These changes in optical properties indicate the importance of considering different types of biomass burning in each location. Wildfire burning events and urban biomass burning might have different characteristic optical properties. Wildfire generated aerosols measured by Lack et al. were also aged, but it might be predominantly organic aerosols in the plume. Also the background conditions for the Lack et al. study are relatively clean compared to polluted regions inside IGP.

Effect of Biomass Burning on Direct Radiative Forcing. Diurnal variation shows that a considerable portion of OA follows the total absorption. Since the amount of OA is much higher than BC in the atmosphere (three times in this study), the absorption due to OA needs to be accounted for while calculating the aerosol DRF. Major global DRF studies use emission inventories as model inputs, which may add significant errors in the estimation.[35] Very few studies have been done based on observations.[5,10,36] Various studies calculated aerosol radiative forcing in the IGP using measured and derived aerosol properties.[23,36,37] These studies used the Optical Properties of Aerosol and Clouds (OPAC) package[38] to derive aerosol optical properties. OPAC uses a lower imaginary refractive index for BC (0.42 at 550 nm) as compared to recent studies (0.71 at 550 nm).[2] Besides, OPAC does not distinguish between organic and inorganic

DOI: 10.1021/acs.est.5b03368
Environ. Sci. Technol. 2015, 49, 10474−10481

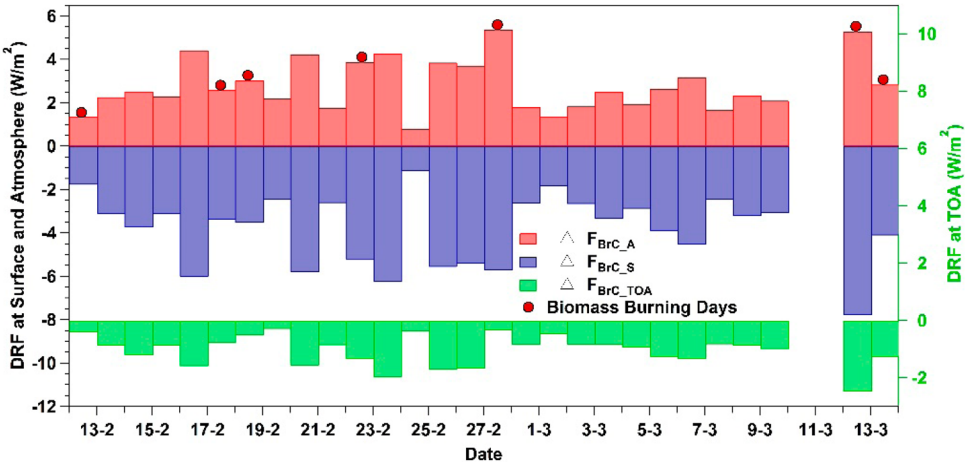

Figure 6. Short wave clear sky BrC aerosol direct radiative forcing for TOA (ΔF_{BrC_TOA}), surface (ΔF_{BrC_S}), and atmosphere (ΔF_{BrC_A}).

aerosols and considers both species as water-soluble species. These factors likely create substantial uncertainty in optical properties derived using OPAC. This study removes such errors by using AERONET derived AOD and g along with surface measured SSA for calculating DRF. Surface measured SSA captures the effect of mixing and BrC absorption and compares closely (within 5%) with columnar SSA from AERONET. Surface SSA measured at 405 and 532 nm has less than 5% difference when compared to AERONET SSA. The difference in SSA at 781 nm is slightly higher (8%) when compared to AERONET SSA. Uncertainty analysis was performed to determine the errors caused by each input parameter (discussed in the SI).

Figure 5 shows the total aerosol ΔF_{TOA}, ΔF_S, and ΔF_A during the study period. Table 2 summarizes the average DRF values. Average values for ΔF_{TOA}, ΔF_S, and ΔF_A are -6.1 ± 3.2, -31.6 ± 11, and $25.5 \pm 10 W/m^2$, respectively. During biomass burning days (shown by red dots in Figure 5), both atmospheric forcing and negative surface forcing increase with respect to normal days. TOA forcing during biomass burning days shows a 32% increase in magnitude, indicating a change from negative to less negative DRF. Average ΔF_{TOA}, ΔF_S, and ΔF_A for normal and biomass burning days are -6.6 ± 2.6, -29.5 ± 9, 22.1 ± 7 W/m^2, and -4.5 ± 4, -38.9 ± 11, and 34.5 ± 12 W/m^2, respectively. Forcing efficiency (ΔF_η) defined as the forcing per unit optical depth, was calculated for TOA level (ΔF_{η_TOA}). Average ΔF_{η_TOA} values for normal and biomass burning days were -22.1 ± 8 and -11 ± 11. Lower values of ΔF_{η_TOA} also indicate the presence of absorbing aerosols.[39] These changes are attributed to the presence of a large amount of BC and BrC emitted to the atmosphere during biomass burning events.

Figure 6 shows the DRF due to BrC alone at TOA (ΔF_{BrC_TOA}), surface (ΔF_{BrC_S}), and atmosphere (ΔF_{BrC_A}). ΔF_{BrC_TOA} and ΔF_{BrC_S} are negative throughout the campaign, whereas ΔF_{BrC_A} was positive. Average values for ΔF_{BrC_TOA}, ΔF_{BrC_S}, and ΔF_{BrC_A} are -1.1 ± 0.5, -3.9 ± 1.6, and 2.8 ± 1.2 W/m^2, respectively. The contribution of BrC to total DRF is found to be 18% at the TOA, 13% at the surface, and 12% in the atmosphere. During biomass burning events, DRF due to BrC follows a similar pattern as that of total DRF. ΔF_{BrC_TOA} shows a positive trend during biomass burning events, which supports results showing less negative DRF values for biomass burning regions by Chung et al.[5] Average ΔF_{BrC_TOA}, ΔF_{BrC_S}, and ΔF_{BrC_A} for normal and biomass burning days are -1.1 ± 0.4, -3.6 ± 1.4, and 2.6 ± 1.0 W/m^2 and -1 ± 0.7, -4.6 ± 1.9, and 3.6 ± 1.5W/m^2, respectively. The difference in average ΔF_{BrC_TOA} during biomass and normal days are insignificant. But ΔF_{BrC_S} values for biomass burning events indicate enhanced reduction in the surface energy balance by 27%, while ΔF_{BrC_A} increases by 40% when compared to respective values of normal days. The combination of enhanced atmospheric absorption combined with a decrease in solar energy reaching the surface suggest that BrC may be having an important influence on atmospheric and surface temperatures and hence climate in the region.

■ ASSOCIATED CONTENT

Supporting Information

This material is available free of charge via the Internet at http://pubs.acs.org/. The Supporting Information is available free of charge on the ACS Publications website at DOI: 10.1021/acs.est.5b03368.

More details on the selection of PMF factors and procedure for calculating the BrC Direct Radiative Forcing values along with error analysis (PDF)

■ AUTHOR INFORMATION

Corresponding Author

*Phone: + 91-512 2597845; e-mail: snt@iitk.ac.in (S.N.T.).

Notes

The authors declare no competing financial interest.

■ ACKNOWLEDGMENTS

The present work is supported by a grant under the Ministry of Human Recourse Development (3-21/2014-TS.1), Government of India. We acknowledge the partial support through U.S. Agency for International Development (AID-OAA-A-11-00012). We also acknowledge the support of IIT Kanpur for providing us with HR-ToF-AMS for PG research and teaching. Antti Arola acknowledge the support from Academy of Finland (project number 264242). Mike Bergin acknowledge partial funding from U.S. EPA grant (R835039), and an NSF PIRE grant (1243535).

DOI: 10.1021/acs.est.5b03368
Environ. Sci. Technol. 2015, 49, 10474−10481

REFERENCES

(1) IPCC, Intergovernmental Panel on Climate Change(IPCC). Climate change 2001. The Scientific Basis, 2001.

(2) Bond, T. C.; Bergstrom, R. W. Light absorption by carbonaceous particles: An investigative review. *Aerosol Sci. Technol.* **2006**, *40* (1), 27−67.

(3) Andreae, M. O.; Gelencsér, A. Black carbon or brown carbon? The nature of light-absorbing carbonaceous aerosols. *Atmos. Chem. Phys.* **2006**, *6* (10), 3131−3148.

(4) Bond; Doherty, S. J.; Fahey, D. W.; Forster, P. M.; Berntsen, T.; DeAngelo, B. J.; Flanner, M. G.; Ghan, S.; Kärcher, B.; Koch, D.; Kinne, S.; Kondo, Y.; Quinn, P. K.; Sarofim, M. C.; Schultz, M. G.; Schulz, M.; Venkataraman, C.; Zhang, H.; Zhang, S.; Bellouin, N.; Guttikunda, S. K.; Hopke, P. K.; Jacobson, M. Z.; Kaiser, J. W.; Klimont, Z.; Lohmann, U.; Schwarz, J. P.; Shindell, D.; Storelvmo, T.; Warren, S. G.; Zender, C. S. Bounding the role of black carbon in the climate system: A scientific assessment. *Journal of Geophysical Research: Atmospheres* **2013**, *118* (11), 5380−5552.

(5) Chung, C. E.; Ramanathan, V.; Decremer, D. Observationally constrained estimates of carbonaceous aerosol radiative forcing. *Proc. Natl. Acad. Sci. U. S. A.* **2012**, *109* (29), 11624−11629.

(6) Kirchstetter, T. W.; Novakov, T.; Hobbs, P. V. Evidence that the spectral dependence of light absorption by aerosols is affected by organic carbon. *J. Geophys. Res.* **2004**, *109* (D21), D21208.

(7) Kanawade, V. P.; Tripathi, S. N.; Bhattu, D.; Shamjad, P. M., Sub-micron particle number size distributions characteristics at an urban location, Kanpur, in the Indo-Gangetic Plain. *Atmos. Res.* **2014***147*−*148*, (0), 121−132.10.1016/j.atmosres.2014.05.010

(8) Shamjad, P. M.; Tripathi, S. N.; Aggarwal, S. G.; Mishra, S. K.; Joshi, M.; Khan, A.; Sapra, B. K.; Ram, K. Comparison of Experimental and Modeled Absorption Enhancement by Black Carbon (BC) Cored Polydisperse Aerosols under Hygroscopic Conditions. *Environ. Sci. Technol.* **2012**, *46* (15), 8082−8089.

(9) Andreae, M. O.; Ramanathan, V. Climate's Dark Forcings. *Science* **2013**, *340* (6130), 280−281.

(10) Liu, J.; Scheuer, E.; Dibb, J.; Ziemba, L. D.; Thornhill, K. L.; Anderson, B. E.; Wisthaler, A.; Mikoviny, T.; Devi, J. J.; Bergin, M.; Weber, R. J. Brown carbon in the continental troposphere. *Geophys. Res. Lett.* **2014**, *41* (6), 2013GL058976.

(11) Virkkula, A.; Mäkelä, T.; Hillamo, R.; Yli-Tuomi, T.; Hirsikko, A.; Hämeri, K.; Koponen, I. K. A Simple Procedure for Correcting Loading Effects of Aethalometer Data. *J. Air Waste Manage. Assoc.* **2007**, *57* (10), 1214−1222.

(12) Weingartner, E.; Saathoff, H.; Schnaiter, M.; Streit, N.; Bitnar, B.; Baltensperger, U. Absorption of light by soot particles: determination of the absorption coefficient by means of aethalometers. *J. Aerosol Sci.* **2003**, *34* (10), 1445−1463.

(13) Arnott, W. P.; Moosmuller, H.; Rogers, C. F.; Jin, T. F.; Bruch, R. Photoacoustic spectrometer for measuring light absorption by aerosol: instrument description. *Atmos. Environ.* **1999**, *33* (17), 2845−2852.

(14) Lack, D. A.; Lovejoy, E. R.; Baynard, T.; Pettersson, A.; Ravishankara, A. R. Aerosol Absorption Measurement using Photoacoustic Spectroscopy: Sensitivity, Calibration, and Uncertainty Developments. *Aerosol Sci. Technol.* **2006**, *40* (9), 697−708.

(15) DeCarlo, P. F.; Kimmel, J. R.; Trimborn, A.; Northway, M. J.; Jayne, J. T.; Aiken, A. C.; Gonin, M.; Fuhrer, K.; Horvath, T.; Docherty, K. S.; Worsnop, D. R.; Jimenez, J. L. Field-Deployable, High-Resolution, Time-of-Flight Aerosol Mass Spectrometer. *Anal. Chem.* **2006**, *78* (24), 8281−8289.

(16) Langridge, J. M.; Richardson, M. S.; Lack, D. A.; Brock, C. A.; Murphy, D. M. Limitations of the Photoacoustic Technique for Aerosol Absorption Measurement at High Relative Humidity. *Aerosol Sci. Technol.* **2013**, *47* (11), 1163−1173.

(17) Huffman, J. A.; Jayne, J. T.; Drewnick, F.; Aiken, A. C.; Onasch, T.; Worsnop, D. R.; Jimenez, J. L. Design, Modeling, Optimization, and Experimental Tests of a Particle Beam Width Probe for the Aerodyne Aerosol Mass Spectrometer. *Aerosol Sci. Technol.* **2005**, *39* (12), 1143−1163.

(18) Singh, R. P.; Dey, S.; Tripathi, S. N.; Tare, V.; Holben, B. Variability of aerosol parameters over Kanpur, northern India. *Journal of Geophysical Research: Atmospheres* **2004**, *109* (D23), D23206.

(19) Canagaratna, M. R.; Jayne, J. T.; Jimenez, J. L.; Allan, J. D.; Alfarra, M. R.; Zhang, Q.; Onasch, T. B.; Drewnick, F.; Coe, H.; Middlebrook, A.; Delia, A.; Williams, L. R.; Trimborn, A. M.; Northway, M. J.; DeCarlo, P. F.; Kolb, C. E.; Davidovits, P.; Worsnop, D. R. Chemical and microphysical characterization of ambient aerosols with the aerodyne aerosol mass spectrometer. *Mass Spectrom. Rev.* **2007**, *26* (2), 185−222.

(20) Ulbrich, I. M.; Canagaratna, M. R.; Zhang, Q.; Worsnop, D. R.; Jimenez, J. L. Interpretation of organic components from Positive Matrix Factorization of aerosol mass spectrometric data. *Atmos. Chem. Phys.* **2009**, *9* (9), 2891−2918.

(21) Ricchiazzi, P.; Yang, S.; Gautier, C.; Sowle, D. SBDART: A Research and Teaching Software Tool for Plane-Parallel Radiative Transfer in the Earth's Atmosphere. *Bull. Am. Meteorol. Soc.* **1998**, *79* (10), 2101−2114.

(22) Stamnes, K.; Tsay, S. C.; Wiscombe, W.; Jayaweera, K. Numerically stable algorithm for discrete-ordinate-method radiative transfer in multiple scattering and emitting layered media. *Appl. Opt.* **1988**, *27* (12), 2502−2509.

(23) Dey, S.; Tripathi, S. N. Estimation of aerosol optical properties and radiative effects in the Ganga basin, northern India, during the wintertime. *J. Geophys. Res.* **2007**, *112* (D3), D03203.

(24) Bergstrom, R. W.; Russell, P. B.; Hignett, P. Wavelength Dependence of the Absorption of Black Carbon Particles: Predictions and Results from the TARFOX Experiment and Implications for the Aerosol Single Scattering Albedo. *J. Atmos. Sci.* **2002**, *59* (3), 567−577.

(25) Bohren, C. F.; Huffman, D. R. Introduction. In *Absorption and Scattering of Light by Small Particles*; Wiley-VCH Verlag GmbH: Weinheim, 2007; pp 1−11.

(26) Bond, T. C.; Habib, G.; Bergstrom, R. W. Limitations in the enhancement of visible light absorption due to mixing state. *J. Geophys. Res.* **2006**, *111* (D20), D20211.

(27) Mätzler, C. MATLAB Functions for Mie Scattering and Absorption. *Institut für Angewandte Physik, Research Report No. 2002*−*08*; Bern, Switzerland, 2002.

(28) Bikkina, S.; Sarin, M. M. Light absorbing organic aerosols (brown carbon) over the tropical Indian Ocean: impact of biomass burning emissions. *Environ. Res. Lett.* **2013**, *8* (4), 044042.

(29) Russell, P. B.; Bergstrom, R. W.; Shinozuka, Y.; Clarke, A. D.; DeCarlo, P. F.; Jimenez, J. L.; Livingston, J. M.; Redemann, J.; Dubovik, O.; Strawa, A. Absorption Angstrom Exponent in AERONET and related data as an indicator of aerosol composition. *Atmos. Chem. Phys.* **2010**, *10* (3), 1155−116.

(30) Lack, D. A.; Langridge, J. M. On the attribution of black and brown carbon light absorption using the Ångström exponent. *Atmos. Chem. Phys.* **2013**, *13* (20), 10535−10543.

(31) Jimenez, J. L.; Canagaratna, M. R.; Donahue, N. M.; Prevot, A. S. H.; Zhang, Q.; Kroll, J. H.; DeCarlo, P. F.; Allan, J. D.; Coe, H.; Ng, N. L.; Aiken, A. C.; Docherty, K. S.; Ulbrich, I. M.; Grieshop, A. P.; Robinson, A. L.; Duplissy, J.; Smith, J. D.; Wilson, K. R.; Lanz, V. A.; Hueglin, C.; Sun, Y. L.; Tian, J.; Laaksonen, A.; Raatikainen, T.; Rautiainen, J.; Vaattovaara, P.; Ehn, M.; Kulmala, M.; Tomlinson, J. M.; Collins, D. R.; Cubison, M. J.; Dunlea, J.; Huffman, J. A.; Onasch, T. B.; Alfarra, M. R.; Williams, P. I.; Bower, K.; Kondo, Y.; Schneider, J.; Drewnick, F.; Borrmann, S.; Weimer, S.; Demerjian, K.; Salcedo, D.; Cottrell, L.; Griffin, R.; Takami, A.; Miyoshi, T.; Hatakeyama, S.; Shimono, A.; Sun, J. Y.; Zhang, Y. M.; Dzepina, K.; Kimmel, J. R.; Sueper, D.; Jayne, J. T.; Herndon, S. C.; Trimborn, A. M.; Williams, L. R.; Wood, E. C.; Middlebrook, A. M.; Kolb, C. E.; Baltensperger, U.; Worsnop, D. R. Evolution of Organic Aerosols in the Atmosphere. *Science* **2009**, *326* (5959), 1525−1529.

(32) Cubison, M. J.; Ortega, A. M.; Hayes, P. L.; Farmer, D. K.; Day, D.; Lechner, M. J.; Brune, W. H.; Apel, E.; Diskin, G. S.; Fisher, J. A.; Fuelberg, H. E.; Hecobian, A.; Knapp, D. J.; Mikoviny, T.; Riemer, D.; Sachse, G. W.; Sessions, W.; Weber, R. J.; Weinheimer, A. J.; Wisthaler, A.; Jimenez, J. L. Effects of aging on organic aerosol from

DOI: 10.1021/acs.est.5b03368
Environ. Sci. Technol. 2015, 49, 10474−10481

open biomass burning smoke in aircraft and laboratory studies. *Atmos. Chem. Phys.* **2011**, *11* (23), 12049−12064.
(33) Lack, D. A.; Langridge, J. M.; Bahreini, R.; Cappa, C. D.; Middlebrook, A. M.; Schwarz, J. P. Brown carbon and internal mixing in biomass burning particles. *Proc. Natl. Acad. Sci. U. S. A.* **2012**, *109*, 14802.
(34) Bougiatioti, A.; Stavroulas, I.; Kostenidou, E.; Zarmpas, P.; Theodosi, C.; Kouvarakis, G.; Canonaco, F.; Prévôt, A. S. H.; Nenes, A.; Pandis, S. N.; Mihalopoulos, N. Processing of biomass-burning aerosol in the eastern Mediterranean during summertime. *Atmos. Chem. Phys.* **2014**, *14* (9), 4793−4807.
(35) Stier, P.; Seinfeld, J. H.; Kinne, S.; Boucher, O. Aerosol absorption and radiative forcing. *Atmos. Chem. Phys.* **2007**, *7* (19), 5237−5261.
(36) Jai Devi, J.; Tripathi, S. N.; Gupta, T.; Singh, B. N.; Gopalakrishnan, V.; Dey, S. Observation-based 3-D view of aerosol radiative properties over Indian Continental Tropical Convergence Zone: implications to regional climate. *Tellus B* **2011**, *63* (5), 971−989.
(37) Dey, S.; Tripathi, S. N. Aerosol direct radiative effects over Kanpur in the Indo-Gangetic basin, northern India: Long-term (2001−2005) observations and implications to regional climate. *J. Geophys. Res.* **2008**, *113* (D4), D04212.
(38) Hess, M.; Koepke, P.; Schult, I. Optical Properties of Aerosols and Clouds: The Software Package OPAC. *Bull. Am. Meteorol. Soc.* **1998**, *79* (5), 831−844.
(39) García, O. E.; Díaz, J. P.; Expósito, F. J.; Díaz, A. M.; Dubovik, O.; Derimian, Y.; Dubuisson, P.; Roger, J. C. Shortwave radiative forcing and efficiency of key aerosol types using AERONET data. *Atmos. Chem. Phys.* **2012**, *12* (11), 5129−5145.

DOI: 10.1021/acs.est.5b03368
Environ. Sci. Technol. 2015, 49, 10474−10481